

# Modeling and Simulation of Membrane Contactor Employed to Strip CO<sub>2</sub> from Rich Solvents via COMSOL Multiphysics®

N.Ghasem<sup>\*1</sup>, M.Al-Marsouqi<sup>1</sup>, and N. Abdul Rahim<sup>1</sup>

<sup>1</sup>United Arab Emirates University

\*Corresponding author: Department of Chemical & Petroleum Engineering, Al-Ain, P. O. Box 15551, UAE, [nayef@uaeu.ac.ae](mailto:nayef@uaeu.ac.ae)

**Abstract:** A mathematical model is developed for the stripping purpose of carbon dioxide from rich solvent. The rich solvent is used in CO<sub>2</sub> absorption from natural gas through gas-liquid hollow fiber membrane contactors. The polyvinylidene fluoride (PVDF) hollow fiber membrane was fabricated via thermally induced phase separation techniques. COMSOL Multiphysics software package is used in solving the set of partial, ordinary and algebraic equations. The model development is based on "non-wetted mode" in which the gas mixture filled the membrane pores for countercurrent gas-liquid contact. Axial and radial diffusion inside the hollow fiber membrane, through the membrane skin, and within the shell side of the contactor is considered in the model. In lab made polyvinylidene fluoride (PVDF) membrane contactor is used in absorption and stripping purposes. The effect of inlet gas and liquid temperature on the membrane performance is investigated. The effect of module packing factor was also investigated. The model predictions obtained via COMSOL is compared with experimental data and is found to be in acceptable range.

**Keywords:** COMSOL, modeling, simulation, membrane contactor, CO<sub>2</sub> stripping.

## 1. Introduction

Hollow fiber membrane is a potential and promising techniques used in the stripping of CO<sub>2</sub> from rich solvents [1, 2]. Among these methods, the most well established method is to separate CO<sub>2</sub> from rich solvent is by conventional stripping conventional contactor equipment such as packed or tray columns [3]. In packed towers or columns, CO<sub>2</sub> contacts the absorbent to form a weak complex and the aqueous solution is then transferred to a regenerating unit to release CO<sub>2</sub> by heating. After this, the solution is cooled and recirculated to the absorption equipment. Although

chemical absorption technology has large commercial significance, the technology is energy-consuming and not easy to operate because of some frequent problems including foaming, flooding, channeling and entrainment.

Membrane gas absorption technology uses hollow fiber membrane contactors to absorb CO<sub>2</sub> from flue gas into solvent. By contrast, chemical absorption technology uses random or structured packed columns to capture CO<sub>2</sub> from flue gas into solvent. Hydrophobic microporous membranes are used to form a permeable barrier between the liquid and gas phases; Absorbent liquid offers the CO<sub>2</sub> selectivity; liquid phase and gas phase are not directly contacted; main driving force is the differential concentration of CO<sub>2</sub> between gas phase and liquid phase; membrane pores must be completely filled by gas.

Liquid phase and gas phase are not directly contacted. Avoid the conventional problems such as flooding, foaming, channeling and entrainment in packed column. Membrane device has larger contact area. Reduction over 70% in size and 66% in weight compared with conventional columns. The interfacial area is known and constant. It does not depend on the operating conditions such as temperature and liquid flow rate. As a result, it is easier to predict the performance of a membrane contactor [4].

Potential problems of membrane gas absorption are membrane wetting. Main difficulty is how to prevent the membrane wetting in the long-term operations. This can be achieved by using hydrophobic membranes through surface modification of membrane, composite membrane, selection of denser hollow fiber membrane; selection of liquid with suitable surface tension and optimizing the operating conditions.

An amino acid salt sodium hydroxide was found to have high tension, high reactivity with CO<sub>2</sub>, and chemical compatibility with membrane material and easiness of regeneration [5-11].

## 2. Use of COMSOL Multiphysics

A steady state mathematical model that described the material balance has been carried out on a shell-and-tube membrane contactor system (Figure 1)

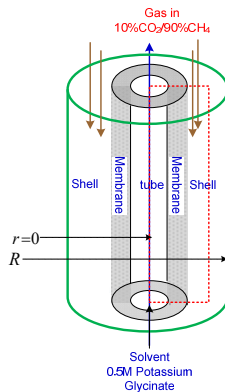


**Figure 1.** Schematic diagram of the hollow fiber section used in modeling the membrane contactor

The model is developed for a segment of a hollow fiber, as shown in Fig. 4, through which the solvent flows with a fully developed laminar parabolic velocity profile. The fiber is surrounded by a laminar gas flow in an opposite direction to that of the liquid. Based on Happel's free surface model [12], only portion of the fluid surrounding the fiber is considered which may be approximated as circular cross section. Thus, symmetry may be considered at the outer portion of the fluid surrounding the fiber (at  $r = r_3$ ). The steady state continuity equation for each species during the simultaneous mass transfer and chemical reaction in a reactive absorption system can be expressed as:

### 2.1 Shell side (gas phase)

The steady state material balance for the transport of gas mixture in the shell side may be written as follows ( $i = \text{CO}_2$  and  $\text{N}_2$ ):

$$D_{i,s} \left[ \frac{1}{r} \frac{\partial}{\partial r} \left( r \frac{\partial C_{i,s}}{\partial r} \right) + \frac{\partial^2 C_{i,s}}{\partial z^2} \right] = \frac{\partial}{\partial z} (V_{zs} C_{i,s}) + \frac{1}{r} \frac{\partial}{\partial r} (r v_{rs} C_{i,s})$$

Considering the active area around each fiber calculated from the hypothetical radius bearing in

mind a hexagonal-shaped unit cell of the fiber assembly around each fiber.

$$r_3 = \frac{r_2}{\sqrt{1-\phi}}$$

where  $\phi$  is the volume void fraction of the membrane contactor module. Assuming Happel's free surface model, the boundary conditions:

$$r = r_2, C_{i,s} = C_{i,m}$$

$$r = r_3, -\frac{\partial C_{i,s}}{\partial r} = 0$$

$$z = 0, -\frac{\partial C_{i,s}}{\partial z} = 0$$

$$z = L, C_{\text{CO}_2,s} = C_{\text{CO}_2}^0, C_{\text{CH}_4,s} = C_{\text{CH}_4}^0$$

### 2.2 Membrane section

The steady state material balance for the transport of  $\text{CO}_2$  and  $\text{N}_2$  across the membrane skin layer for non-wetting mode of operation is considered to be due to diffusion only; no reactions are taking place in the gas filled pores ( $i = \text{CO}_2$  and  $\text{N}_2$ ).

$$D_{i,m} \left[ \frac{\partial^2 C_{i,m}}{\partial r^2} + \frac{1}{r} \frac{\partial C_{i,m}}{\partial r} + \frac{\partial^2 C_{i,m}}{\partial z^2} \right] = 0$$

Boundary conditions:

$$r = r_1, C_{i,m} = C_{i,t} / m_i$$

$$r = r_2, C_{i,m} = C_{i,s}$$

$$z = 0, z = L, \frac{\partial C_{i,m}}{\partial z} = 0$$

where  $m_i$  is the solubility of  $\text{CO}_2$  and  $\text{N}_2$  in aqueous sodium hydroxide solution.

### 2.3 Tube Side (liquid phase)

The steady state material balance for the transport of  $\text{CO}_2$  and aqueous  $\text{NaOH}$  in the lumen side of the hollow fiber membrane tubes is considered to be due to diffusion, convection and reaction as well:

$$D_{i,t} \left[ \frac{1}{r} \frac{\partial}{\partial r} \left( r \frac{\partial C_{i,t}}{\partial r} \right) + \frac{\partial^2 C_{i,t}}{\partial z^2} \right] + r_{i,t} = \frac{\partial}{\partial z} (v_{zt} C_{i,t}) + \frac{1}{r} \frac{\partial}{\partial r} (r v_{rt} C_{i,t})$$

where the subscript "i" indicates carbon dioxide and sodium hydroxide.

### Boundary conditions:

The boundary conditions for liquid flowing in lumen side of the fibers ( $i = \text{CO}_2$  and  $\text{NaOH}$ ):

$$r = 0, \quad -\frac{\partial C_{i,t}}{\partial r} = 0$$

$$r = r_1, \quad C_{i,t} = m_i C_{i,m}$$

$$z = 0, \quad C_{\text{NaOH},t} = C_{\text{NaOH}}^\circ$$

$$z = L, \quad -\frac{\partial C_{i,t}}{\partial z} = 0$$

### 2.4 Energy balance

#### Shell side

The steady state energy balance equations for shell side, membrane section and tube side are developed as follows (No reaction is taking place in the shell gas side):

$$\rho_g C_{pg} \left( v_{rs} \frac{\partial T_s}{\partial r} + v_{zs} \frac{\partial T_s}{\partial z} \right) = k_g \left[ \frac{1}{r} \frac{\partial}{\partial r} \left( r \frac{\partial T_s}{\partial r} \right) + \frac{\partial^2 T_s}{\partial z^2} \right]$$

Boundary conditions:

$$r = r_2, \quad T_s = T_m,$$

$$r = r_3, \quad \frac{\partial T_s}{\partial r} = 0,$$

$$z = 0, \quad \frac{\partial T_s}{\partial z} = 0$$

$$z = L, \quad T_s = T_{0,g}$$

#### Membrane section

Accordingly, the steady state thermal energy equation for the gas and membrane that are at the thermal equilibrium conditions, is simplified to

$$0 = \left[ k_m \frac{1}{r} \frac{\partial}{\partial r} \left( r \frac{\partial T_m}{\partial r} \right) + k_m \frac{\partial^2 T_m}{\partial z^2} \right]$$

Boundary conditions:

$$r = r_1, \quad -k_t \frac{\partial T_t}{\partial r} = -k_m \frac{\partial T_m}{\partial r}$$

$$r = r_2, \quad T_m = T_s,$$

$$z = 0, \quad z = L, \quad -\frac{\partial T_s}{\partial z} = 0$$

#### Tube side (Liquid phase):

In the tube side heat is transferred through, conduction, convection and through solvent evaporation as well.

$$\rho_L C_{pL} \left( v_{rt} \frac{\partial T_t}{\partial r} + v_{zt} \frac{\partial T_t}{\partial z} \right) = k_L \left[ \frac{1}{r} \frac{\partial}{\partial r} \left( r \frac{\partial T_t}{\partial r} \right) + \frac{\partial^2 T_t}{\partial z^2} \right]$$

Boundary conditions:

$$r = 0, \quad -\frac{\partial T_t}{\partial r} = 0,$$

$$r = r_1, \quad -k_t \frac{\partial T_t}{\partial r} = -k_m \frac{\partial T_m}{\partial r}$$

$$z = 0, \quad T_t = T_{t,0},$$

$$z = L, \quad -\frac{\partial T_t}{\partial z} = 0$$

More details and the parameters used in the simulation can be found elsewhere [12]. The simultaneous partial differential equations were solved using software COMSOL Multiphysics.

### 3. Experimental

The schematic diagram of the experimental setup used in  $\text{CO}_2$  absorption is shown in Figure 2. In this experiment the effect of inlet absorbent temperature on system performance is investigated. Inlet and exit temperatures of the liquid and gas streams were measured using temperature sensors located at the inlet and exit of both liquid and gas streams. The water evaporated from the absorbent liquid at various absorbent inlet temperatures is condensed and collected using refrigerated cooling water bath and condenser. The gas free water vapor is sent to the gas chromatography (GC). The gas GC is used to measure the  $\text{CO}_2$  concentration in the exit gas stream. The amount of condensed water vapor is weighed using high precision digital balance placed under the collecting vessel.

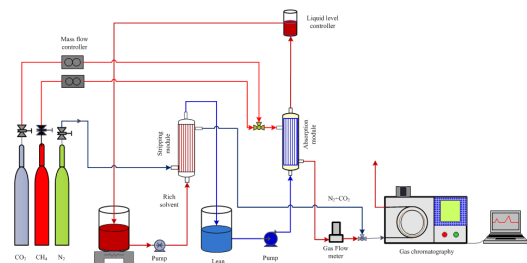
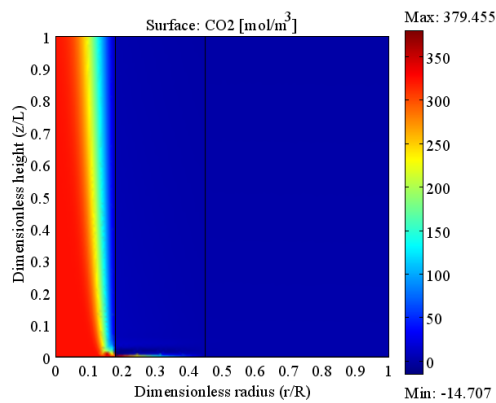


Figure 2. Schematic diagram of  $\text{CO}_2$  stripping unit

#### 4. Results and Discussion

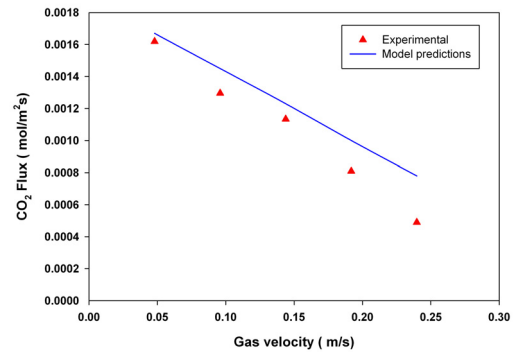
The surface diagram generated for the set of model equations generated from the mass balance around the membrane module was solved via COMSOL software package and depicted in Figure 3. The diagram depicts the CO<sub>2</sub> concentration across the membrane module. The diagram revealed around 80% removal of carbon dioxide is stripped within the membrane length as shown from the blue color on the shell side, as the gas (nitrogen) is entering counter currently with liquid solvent (0.5 M sodium hydroxide with absorbed CO<sub>2</sub>).



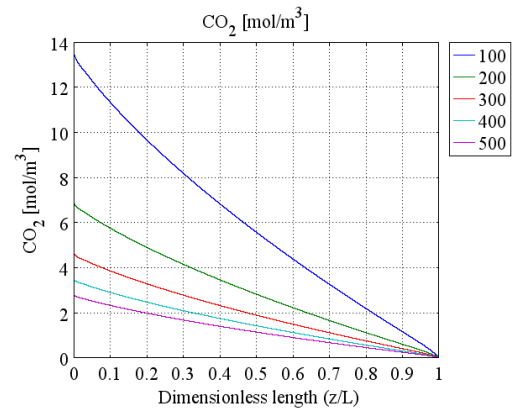
**Figure 3.** Surface plot for CO<sub>2</sub> stripping from aqueous solvent via a membrane contactor

Figure 4 shows a comparison between experiment results and model prediction at various inlet solvent temperatures. The results revealed that carbon dioxide removal flux increased with increased solvent inlet temperature. That is attributed to increased rate constant with temperature, hence, increased reaction rate removal flux.

The concentration of carbon dioxide in stripped gas nitrogen is shown in Figure 5. The concentration of the carbon dioxide in the stripped nitrogen gas flowing in the shell side decreased with increased stripped gas flow rate. This trend is expected since the residence time decreases with increases of stripped gas flow rate.



**Figure 4.** Effect of sodium hydroxide temperature on CO<sub>2</sub> removal flux



**Figure 5.** Effect of sweep gas (nitrogen) flow rate on the concentration of CO<sub>2</sub>

#### 5. Conclusions

PVDF hollow fiber membrane was fabricated successfully via thermally induced phase separation. The in-house fabricated membrane was utilized as gas-liquid membrane contactor module. The constructed module was used for the stripping of CO<sub>2</sub> from aqueous sodium hydroxide solvent used in natural gas absorption using sodium hydroxide solvent. A round 70% removal was achieved using sodium hydroxide as solvent. The model prediction and experimental results were in acceptable trend with model prediction.

## 6. Nomenclature

$A$	Total area of membrane, m <sup>2</sup>
$C_i$	Concentration of component $i$
$C_{i,m}$	Concentration of component $i$
$C_{i,s}$	Concentration of component $i$
$C_{i,t}$	Concentration of component $i$
$D_i$	Diffusion coefficient of component
$d_p$	Pore diameter, m
$d_m$	Module diameter, m
$h_m$	Mass transfer coefficient, m s <sup>-1</sup>
$k_m$	Thermal conductivity of solid
$k_g$	Gas filled pores thermal conductivity
$L$	Length of hollow fiber membrane, m
$m$	Physical solubility
$p$	Pressure, Pa
$r_1$	Inner tube radius, m
$r_2$	Outer tube radius, m
$r_3$	Estimated module radius, m
$R$	Dimensionless radius, m
$R_g$	Universal gas constant,
$T_m$	Membrane section temperature, K
$T_s$	Shell side temperature, K
$T_t$	Tube side temperature, K
$v_{ot}$	Solvent inlet velocity it tube side, m s <sup>-1</sup>
$v_{os}$	gas side inlet velocity it tube side, m s <sup>-1</sup>
$v_r$	Velocity of fluid inside the module
$v_z$	Velocity of fluid inside the
$z$	Axial distance, m

### Greek letters

$\rho$	Gas density, g cm <sup>-3</sup>
$\mu$	Viscosity of gas, Pa s
$\varepsilon_s$	Membrane surface porosity
$\mathcal{E}$	Membrane bulk porosity

## 7. References

1. T. O'Brien, Review of novel methods for carbon dioxide separation from flue and fuel gases, *Fuel Process. Technol.* **86**, 1423–1434 (2005)
2. J.-L. Li, B.-H. Chen, Review of CO<sub>2</sub> absorption using chemical solvents hollow fiber

membrane contactors, *Sep. Purif. Technol.* **41**, 109–122. (2005)

3. E.L. Cussler, in: G. Joao, et al., (Eds.), *Hollow Fiber Contactors in membrane Processes in Separation and Purification*, Kluwer Academic Publishers, (1994)
4. Y.-S. Kim, S.-M. Yang, Absorption of carbon dioxide through hollow fiber membranes using various aqueous absorbents, *Sep. Purif. Technol.* **21**,101–109 (2000)
5. Y. Shui-ping. Experimental study on the separation of CO<sub>2</sub> from flue gas using hollow fiber membrane contactors without wetting. *Fuel Processing Technology*, **88**, 501–511 (2007)
6. R. Prasad and K. Sirkar, Dispersion-free solvent extraction with microporous hollow-fiber modules. *AIChE journal.* **34**, 177-88 (2004)
7. A. Xu, Yang, A., S. Young, D. demontignyand P. Tontiwachwuthikul P, Effect of internal coagulant on effectiveness of polyvinylidene fluoride membrane for carbon dioxide separation and absorption. *Journal of Membrane Science.* **311**, 153-8(2008)
8. G. Afraneand, EH. Chimowitz, Experimental investigation of a new supercritical fluid-inorganic membrane separation process. *Journal of Membrane Science.* **116**, 293-9 (1996)
9. Y-W, Chiu, and Tan C-S. Regeneration of supercritical carbon dioxide by membrane at near critical conditions. *The Journal of Supercritical Fluids.* **21**, 81-9 (2001)
10. G.F. Versteeg, and Van Swaaij W. Solubility and diffusivity of acid gases (carbon dioxide, nitrous oxide) in aqueous alkanolamines solutions. *Journal of Chemical and Engineering Data.* **33**, 29-34 (1988)
11. A. Mansourizadeh, Experimental study of CO<sub>2</sub> absorption/stripping via PVDF hollow fiber membrane contactor. *Chemical Engineering Research and Design.* **90**, 555-62 (2012)
12. N. Ghasem, M. Al-Marzouqi, N. Abdul Rahim, Modeling of CO<sub>2</sub> absorption in a membrane contactor considering solvent evaporation, *Separation and Purification Technology* **110**, 1–10 (2013)

## 8. Acknowledgements

The authors would like to thank UAEU Program for Advanced Research (UPAR) 2013 (formally UAEU-NRF Grants program) for the sponsor of our research project no. 25357.